

Wideband Cancellation of Interference in a GPS Receive Array

R. L. FANTE, Fellow, IEEE
J. J. VACCARO
The MITRE Corporation

We have demonstrated that by using an adaptive space-time array the interference from multiple, strong interferers plus multipath can be canceled down close to the noise floor without producing serious loss or distortion of a GPS signal. Design criteria are presented and limitations are examined. We also compare space-time processing with suboptimum space-frequency processing, and demonstrate by simulation that for equal computational complexity space-time processing slightly outperforms suboptimum space-frequency processing.

Manuscript received January 14, 1999; revised June 22 and November 15, 1999; released for publication November 18, 1999.

IEEE Log No. T-AES/36/2/05229.

Refereeing of this contribution was handled by W. D. Blair.

Authors' address: The MITRE Corporation, 202 Burlington Rd., Bedford, MA 01730-1420.

0018-9251/00/\$10.00 © 2000 IEEE

I. NOMENCLATURE

B	Bandwidth
CR	Cancellation ratio
J/N	Interference-to-noise ratio per interferer per element
K	Number of antennas
L	Number of multipath scattering centers
M	Size of fast Fourier transform (FFT) and, therefore, the number of frequency bins
N	Number of interferers
N_r	Number of ripples in $H(f)$ across band B
P	Number of time taps per antenna
Q	Order of suboptimum space-frequency processor
T	Time delay per tap.

II. INTRODUCTION

It is desirable that GPS receivers operate efficiently, even in the presence of interference and interference multipath. In order to counter this problem an adaptive antenna array is required because the location of the interference will not be known, a priori. Conventional adaptive arrays that employ spatial degrees of freedom to place nulls in the direction of interferers perform well over very narrow bandwidths, but may be inadequate for broader band operation, especially when multipath is present. In order to form broadband nulls both spatial and temporal adaptive degrees of freedom are required [1-3], and a generic space-time processor that has the potential to cancel both interferers and their multipath is shown in Fig. 1. This architecture is a special case of the three-dimensional space-time processor (3D STAP) proposed for radar systems to cancel ground clutter, jammers and jammer multipath [3-7]. The adaptive FIR (finite impulse response) filters are able to tailor the response so as to null interference plus multipath over broader bandwidths, provided the time delays T are less than $1/B$, where B is the operating bandwidth, and the length $(P-1)T$ of each adaptive FIR filter is sufficient to encompass the differential multipath delays. The processor works by choosing the adaptive weights w_{kq} so as to preserve the desired GPS signal while simultaneously minimizing all interference. That is, we use the fact that we have information on the angular location of each GPS satellite and the nature of the signal it transmits, to tailor the space-time filter to receive this signal while rejecting others. In the next section we illustrate how this is done for hypothetical antenna arrays.

III. ADAPTIVE FILTER WEIGHTS

We now wish to choose the weights w_{kq} shown in Fig. 1 so as to receive the signal from

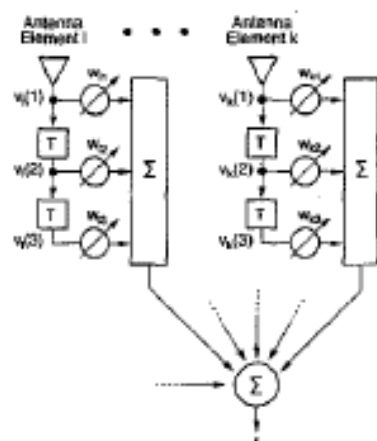


Fig. 1. Adaptive space-time processor with 3 taps per antenna. Frequency transfer function of filter is $H(f)$.

each¹ GPS satellite while at the same time rejecting all other signals. In order to see how this is done refer to Fig. 1. The interferers plus their multipath produce a voltage $y_k(t)$ on antenna k , and this voltage is then received and downconverted, producing a voltage $v_k(t)$ at the input to the FIR filter, and a voltage $v_k(t - qT)$ on time tap q . We then desire to choose a set of weights w_{kq} so that the filter output

$$z(t) = \sum_{k=1}^K \sum_{q=0}^{P-1} w_{kq} v_k(t - qT) \quad (1)$$

preserves the GPS signal while canceling the interference and its multipath. In order to compactly formulate this problem let us define the $KP \times 1$ vector V as

$$V^T = [v_1(0) \dots v_1(P-1) \dots v_K(0) \dots v_K(P-1)] \quad (2)$$

where $v_k(q) = v_k(t - qT)$ is the voltage on time tap q of antenna k produced by the interferers, interference multipath and noise. Also define a $KP \times 1$ weight vector W as

$$W^T = [W_{1,0} \dots W_{1,P-1} \dots W_{K,0} \dots W_{K,P-1}]. \quad (3)$$

Then (1) can be rewritten as

$$z = W^T V. \quad (4)$$

The average interference power at the filter output is

$$\begin{aligned} \langle |z|^2 \rangle &= W^H \langle V^* V^T \rangle W \\ &= W^H R W \end{aligned} \quad (5)$$

where $\langle \rangle$ denotes an expectation and R is the interference-plus-noise covariance matrix. This covariance matrix is derived in Appendix A and includes the effects of system bandwidth, multipath, and channel mismatch. In practice, R is estimated [8]

¹That is, a different set of weights is obtained for each GPS satellite.

by averaging approximately $4KP$ independent time samples of the received interference. Because the GPS signal strength is at least 20 dB below the ambient noise floor, there is no need to be concerned about obtaining signal-free samples.

When the desired GPS signal is incident and signal multipath is absent,² a voltage $s_k(q) \equiv s_k(t - qT)$ is produced on time tap q of antenna k . If we define a $KP \times 1$ vector S as

$$S^T = [s_1(0) \dots s_1(P-1) \dots s_K(0) \dots s_K(P-1)] \quad (6)$$

we see that the signal voltage at the filter output is

$$z_s = W^T S. \quad (7)$$

We now wish to determine the weight vector W . Because S is a stochastic vector (typically the GPS signal is a Gold code or a PN (pseudonoise) sequence) the classical solution [8-13],

$$W = R^{-1} S^*$$

used for deterministic signals is not appropriate, so we now consider some different approaches for calculating W .

A. Maximum Signal-to-Interference Ratio

The average signal power at the filter output can be obtained from (7) as

$$\begin{aligned} \langle |z_s|^2 \rangle &= W^H (S^* S^T) W \\ &= W^H \Gamma W. \end{aligned} \quad (8)$$

We now wish to determine the weight W that maximizes the average signal-to-interference ratio

$$SI = \frac{W^H \Gamma W}{W^H R W}. \quad (9)$$

The desired weight W is readily shown [14] to be the eigenvector that corresponds to the maximum eigenvalue λ of

$$\Gamma W = \lambda R W \quad (10)$$

with the maximum signal-to-interference ratio (ignoring signal multipath) equal to the largest eigenvalue. Note that the process is repeated for each GPS satellite to be used in the solution for the platform position vector.

In practice, signal multipath is not always negligible, so the actual signal is $S_a = S + S_m$, where S_m is the multipath contribution. Then, the ideal signal covariance matrix must be replaced by the actual covariance matrix

$$\Gamma_a = \langle (S^* + S_m^*)(S + S_m)^T \rangle \quad (11)$$

²In reality signal multipath is nearly always present. When the antenna is mounted on a complex structure it is difficult to model the multipath accurately and include it in our assumed signal. Thus, we are forced to assume that the incident signal is composed only of the direct, unscattered component.

and the actual signal-to-interference ratio after adaptation is

$$SI_a = \frac{W^H \Gamma_a W}{W^H R W}. \quad (12)$$

Typically, the signal multipath causes the actual signal-to-interference ratio to be a few tenths of a dB below the ideal value. Of course, the interference covariance matrix R always contains the interference multipath.

B. Minimum Mean Square Error

A second approach is to choose the weight vector to minimize the mean square difference between the desired temporal signal sequence s_d and the total received voltage $W^T Z$, where $Z = V + S$ is the total voltage vector consisting of signal plus all interference. That is, we choose W to minimize

$$\begin{aligned} \epsilon &= \langle |s_d - W^T Z|^2 \rangle \\ &= \langle s_d s_d^* \rangle - W^T \langle Z s_d^* \rangle - W^H \langle Z^* s_d \rangle \\ &\quad + W^H \langle Z^* Z^T \rangle W. \end{aligned} \quad (13)$$

If we differentiate ϵ with respect to W^H , set the result equal to zero and use the information that the GPS signal is independent of and much weaker than the interference-plus-noise we find

$$W = R^{-1} g_s, \quad (14)$$

where

$$g_s = \langle S^* s_d \rangle \quad (15)$$

is the first column of the signal covariance matrix Γ . The signal-to-interference ratio after adaptation is then obtained by using (14) in (12).

The weight vectors in (10) and (14) are not equal, but we have shown elsewhere (using very many typical portions of PN sequences), that the result in (14) gives signal-to-interference ratios that are only a few tenths of a dB less than those given using the weight in (10). Thus, either approach is acceptable, but in the simulations presented in Section VI, (14) has been used.

C. Minimum Output Power

Because the GPS signal is usually far below the receiver noise level, a simple power minimization is often quite useful. In this method we simply constrain the weight on the middle tap of antenna 1 (see Fig. 1), and then minimize the output power without attempting to preserve the gain in the signal direction. This method has the disadvantage of allowing for possible signal fades, but the advantage of not requiring the user to know the expected direction of arrival of the incoming GPS signal. This approach was not pursued in this work.

In our analysis in Subsections A and B it was assumed that the angular location of each GPS satellite in view is approximately known, and that a separate weight vector is calculated to either maximize the signal-to-interference ratio or minimize the mean square error for each satellite. However, because the visible GPS satellites usually lie above the horizon and interference very often comes from at or near the horizon, it is possible to maximize the average of SI over some solid angle Ω_0 (or minimize the average of ϵ), where Ω_0 includes nearly the entire upper hemisphere except the region near the horizon. In this case Γ in (9) is replaced by $\bar{\Gamma}$ and g_s in (15) is replaced by \bar{g}_s , where

$$\begin{aligned} \bar{\Gamma} &= \frac{1}{\Omega_0} \iint_{\Omega_0} d\Omega \langle S^* S^T \rangle \\ \bar{g}_s &= \frac{1}{\Omega_0} \iint_{\Omega_0} d\Omega \langle S^* s_d \rangle \end{aligned}$$

and $d\Omega$ is the element of solid angle. The advantages of this procedure are that a) one no longer needs to know the angular locations of each GPS satellite, and b) a single weight vector is used for all satellites. However, the disadvantage is that we can no longer be assured of achieving full gain at the location of each satellite. In a future paper we will present a detailed tradeoff of individual constraints versus hemisphere-averaged constraints.

IV. SIGNAL DISTORTION INTRODUCED BY THE PROCESSOR

As we see later the processor described in the last section can cancel the interference introduced by ensembles of wideband and narrowband interferers, but because the architecture in Fig. 1 does not have a uniform frequency response across the operating band, it is possible that it will introduce a distortion of the desired GPS signal. In order to study this problem, including steering vector mismatch, suppose the GPS satellite is located at polar angle (θ_s, ϕ_s) and we assume it is at a different angle $(\hat{\theta}_s, \hat{\phi}_s)$. Then, it is readily seen that the response of the filter in Fig. 1 to that satellite is

$$H(f, \theta_s, \phi_s; \hat{\theta}_s, \hat{\phi}_s) = \sum_{k=1}^K \sum_{q=0}^{P-1} \bar{w}_{kq} \exp \left[i2\pi f \left(\frac{\xi_k}{c} + qT \right) \right] \quad (16)$$

where f is the frequency, $\bar{w}_{kq} = w_{kq}(\hat{\theta}_s, \hat{\phi}_s) \cdot \exp(i2\pi f_0 \xi_k / c)$, f_0 is the carrier frequency,

$$\xi_k = x_k \sin \theta_s \cos \phi_s + y_k \sin \theta_s \sin \phi_s + z_k \cos \theta_s, \quad (17)$$

(x_k, y_k, z_k) is the position of antenna k and $w_{kq}(\hat{\theta}_s, \hat{\phi}_s)$ is the weight vector computed for assumed satellite position $(\hat{\theta}_s, \hat{\phi}_s)$. Because $(\hat{\theta}_s, \hat{\phi}_s)$ and the filter weights

w_{kq} are all known (after adaptation), this filter function is readily constructed. If the GPS satellite emits a signal with a Fourier transform $S(f)$, then, in the absence of signal multipath, the signal output after passing through the adaptive filter is $H(f)S(f)$, which can be written in the time domain as

$$r(t) = \int_{-\infty}^{\infty} df H(f) S(f) \exp(i2\pi ft) \quad (18)$$

where, for notational convenience we have suppressed the angular dependence of H . The GPS receiver estimates time delay by using [15, 16] the cross correlation³ of this received signal with the known signal

$$r_0(t) = \int_{-\infty}^{\infty} df' S(f') \exp(i2\pi f't). \quad (19)$$

If the signal is a stationary random process, then

$$\langle S(f)S^*(f') \rangle = P(f)\delta(f-f') \quad (20)$$

where $P(f)$ is the power spectrum of the signal. If (20) is used, along with (18) and (19), we see that the cross correlation is

$$\begin{aligned} C(\tau) &= \langle r(t)r_0^*(t+\tau) \rangle \\ &= \int_{-\infty}^{\infty} df P(f) H(f) \exp(-i2\pi f\tau). \end{aligned} \quad (21)$$

Typically, $P(f)$ is a positive, symmetric function of f , so that in the absence of $H(f)$ the correlation peak occurs at $\tau = 0$. However, $H(f)$ can introduce both a broadening of the correlation peak and a shift of that peak from the correct value at $\tau = 0$. This shift (or bias) is introduced by the phase $\phi(f)$ of $H(f)$. In addition, the presence of $H(f)$ could lead to a phase shift at the value of τ where the correlation peak occurs, and this could affect the high-precision, differential GPS systems that use carrier-phase tracking. Thus, in a later section it is necessary to carefully examine the effect of the adaptive anti-jam filter $H(f)$ on the cross correlation function. Of course, if necessary, both the bias error and any phase shifts, but not the broadening effect, can be corrected by following the adaptive FIR filter with the filter⁴ $G(f) = H^*(f)$. Then, the cross correlation becomes

$$C'(\tau) = \int_{-\infty}^{\infty} df P(f) |H(f)|^2 \exp(-i2\pi f\tau). \quad (22)$$

Because $P(f)|H(f)|^2$ is real, the peak of $|C(\tau)|$ now lies at the correct location ($\tau = 0$) and, clearly, the phase of $C'(0)$ is zero, as desired. However, the

correlation peak can potentially be broadened. Thus, there will be no bias in the pseudorange⁵ estimate, but the standard deviation of the error in the estimated platform location may be increased. In a later section we show that this compensation filter $G(f)$ is rarely needed. Unfortunately the compensation filter $H^*(f)$ does not cure the range estimation problems caused by signal multipath. Signal multipath causes [17] the correct GPS signal transform $S(f)$ to be replaced by $S(f)(1 + \Delta(f))$, where Δ is of the form

$$\Delta(f) = \sum_{r=1}^{R_m} a_r \exp(-i2\pi f\tau_r) \quad (23)$$

and R_m is the number of multipath sources, and a_r , τ_r are the strength and delay of each multipath scatterer, respectively. Note that because the GPS satellite is at a different location than the interferers, the signal multipath delays are different than the interferer multipath delays. In the presence of signal multipath, (22) is replaced by

$$C'(\tau) = \int_{-\infty}^{\infty} df P(f) |H(f)|^2 [1 + \Delta(f)] \exp(-i2\pi f\tau). \quad (24)$$

Unless $\Delta(f)$ is quite small it is evident from (24) that the signal multipath can introduce both a bias and a broadening of the correlation peak.

V. SUBOPTIMUM SPACE-FREQUENCY PROCESSING

We now wish to explore a suboptimum approach [18] that may possibly reduce the computational complexity without greatly sacrificing performance. One method that readily suggests itself is to process in the frequency rather than the time domain. That is, perhaps we can split the operating band B into M subbands of bandwidth B/M , and then in each subband calculate weights for each antenna that cancels the interference by placing spatial nulls on interferers within that bin while preserving the signal. If the discrete Fourier transform (implemented as a fast Fourier transform (FFT)) really did behave as a "brick wall" filter bank that fully isolated each frequency bin from all others, we expect that this procedure would rival the full time-domain processing discussed earlier. However, because of leakage between bins, even with well-designed windows, it is necessary to consider what is happening in some adjacent bins when attempting to minimize interference in a particular frequency bin. We now discuss a method for accounting for this spillover among bins.

³This is referred to in GPS literature as the "code tracking loop."

⁴It should be recognized that $G(f) = H^*(f)$ is not the only option for compensation. In fact the filter $G(f) = H^*(f)/|H(f)|^2$ is preferable because the cross correlation $C'(\tau)$ after compensation is then undistorted. However, whereas $H(f)$ is a simple FIR filter, $G(f)$ is not.

⁵Because the GPS satellite and receiver clocks are not identical, a GPS system does not measure true range, but rather pseudo-range. If the same clock were used then the differential delay would yield true range.

Before we proceed to discuss this approach let us first transform the data into the frequency domain as

$$X_n(m) = \sum_{k=0}^{M-1} b(k)x_n(k) \exp\left(j\frac{2\pi mk}{M}\right) \quad (25)$$

where $b(k)$ is an arbitrary windowing function (e.g., Hamming), $x_n(k)$ is the voltage on time tap k of antenna n and $X_n(m)$ is the voltage in frequency bin m of antenna n . We combine these components into an $KM \times 1$ frequency-domain voltage vector X as

$$X^T = [X_1(0) \dots X_K(0) X_1(1) \dots X_K(1) \dots X_1(m) \dots X_K(m) \dots] \quad (26)$$

where K is the number of antennas. Next, we define a $KM \times 1$ weight vector $W_Q(m)$ for order Q processing as

$$W_1(m)^T = [0 \dots 0 w_1(m) \dots w_K(m) 0 \dots 0] \quad (27)$$

$$W_2(m)^T = [0 \dots 0 w_1(m) \dots w_K(m) w_1(m+1) \dots w_K(m+1) 0 \dots 0] \quad (28)$$

$$W_3(m)^T = [0 \dots 0 w_1(m-1) \dots w_K(m-1) w_1(m) \dots w_K(m) w_1(m+1) \dots w_K(m+1) 0 \dots 0]. \quad (29)$$

Then, for an arbitrary order Q the output in frequency bin m after applying the weights to the data is

$$V_Q(m) = W_Q^T(m)X. \quad (30)$$

Thus, for first order processing, defined by $Q = 1$, the output after weighting in frequency bin m is given by

$$V_1(m) = \sum_{n=1}^K w_n(m)X_n(m) \quad (31)$$

which clearly shows that bin m is processed without regard for the voltage in the other bins. Second-order processing, defined by $Q = 2$, gives

$$V_2(m) = \sum_{n=1}^K [w_n(m)X_n(m) + w_n(m+1)X_n(m+1)] \quad (32)$$

and for third-order ($Q = 3$) processing we have

$$V_3(m) = \sum_{n=1}^K [w_n(m-1)X_n(m-1) + w_n(m)X_n(m) + w_n(m+1)X_n(m+1)] \quad (33)$$

etc. Thus, as we increase the order Q we increasingly account for the data in other bins when calculating the output in a given bin m . Consequently, we expect that

as the order is increased we can improve our ability to cancel the interference in each bin while preserving the desired signal there. In the limit when the filter order Q equals the number of taps, it can be shown [19] that space-frequency and space-time processing are equivalent.

For filter order Q , the unknown weights in (31)–(33) are computed by minimizing the mean square difference between the actual voltage $V_Q(m)$ in bin m and the Fourier transform $S_d(m)$ of the desired signal. The procedure parallels the approach of DiPietro [18], and is omitted here (complete details are contained in [20]). In a later section we compare suboptimum space-frequency processing with full space-time processing to see if space-frequency processing really offers any computational advantages.

VI. NUMERICAL SIMULATIONS

A. Introduction

We now wish to evaluate the cancellation performance of the full order space-time processor described in Section III and of the suboptimum space-frequency processor described in Section V. We assume a priori that the receiver in Fig. 1 contains an analog-to-digital converter (A/D) with sufficient dynamic range to encompass the interference-to-noise ratio. We also assume that each receiver has a response that is essentially linear over the range of operation. If one specifies that, in the presence of a jammer nonlinearity, variations from receiver-to-receiver produce less than a 1 dB increase in output interference this leads to the requirement [20] that

$$|\beta_n - \beta_m| < \frac{0.47}{J \left(\frac{J}{N}\right)^{1/2}} \quad (34)$$

where J is the interferer power, J/N is the interference-to-noise ratio and β_n, β_m are the cubic nonlinearity coefficients of receivers n and m , respectively.

For our first set of simulations we consider a seven-element planar array with elements uniformly

spaced around a circle of radius equal to one-half wavelength, assume that the operating frequency is 1.575 GHz (L1) and that the operating bandwidth is 20 MHz. In the absence of multipath the adaptive tapped delay lines shown in Fig. 1 are probably unnecessary except for very strong interferers, because the maximum delay across the array in Fig. 3 is only 0.67 ns. Thus, the product of the bandwidth and this delay is only $0.67 \times 10^{-9} \times 20 \times 10^6 = 0.013$. However, when the array is placed on a platform the maximum differential multipath delay can be of order of 100 ns and the delay-bandwidth product then is of order 2, so that the tapped delay lines are clearly necessary. In fact, $B\tau$ products as small as a few tenths produce significant degradation if only spatial nulling is used.

Our simulation accounts for antenna cross-polarization, mutual coupling between antennas and mismatch between the different antenna responses. We have found that for $P > 1$ mutual coupling has virtually no effect⁶ on the results unless the mutual coupling coefficient is greater than -15 dB. For nearly all arrays of interest, the mutual coupling is well below this value. In the results to be presented the mutual coupling option was ignored in order to save computer time. The antenna mismatch, however, is an extremely important parameter, and we have expressed the antenna mismatch in terms of a quantity known as the "cancellation ratio," which is minus the logarithm of the normalized residue power when two antennas are illuminated by the same interferer and their outputs subtracted. A high cancellation ratio means that the channels are well matched and a low cancellation ratio implies poorly matched receivers. A derivation of the cancellation ratio in terms of the amplitude and phase mismatch across the operating band is presented in Appendix A.

The multipath is modeled as a set of point scatterers with an arbitrary strength and position. The strength is defined relative to the strength of the direct ray from the interferer. Thus, a strength of -40 dB means that the multipath produces a voltage on each element that is 0.01 of the voltage produced by the direct signal from the interferer. Additional details on the multipath model are given in Appendix A.

Let us first examine how multipath affects interferer cancellation. We consider the processor in Fig. 1 and assume that the array is illuminated by an array of interferers located randomly in azimuth near the horizon (x-y plane). The GPS satellite is assumed to be located 10° off array boresight and the multipath is modeled by four point scatterers located at (d, d) , $(d, -d)$, $(-d, d)$, $(-d, -d)$. Thus, for

⁶For $P = 1$ (no time taps) mutual coupling significantly affects the results if the coupling coefficient exceeds approximately -30 dB.

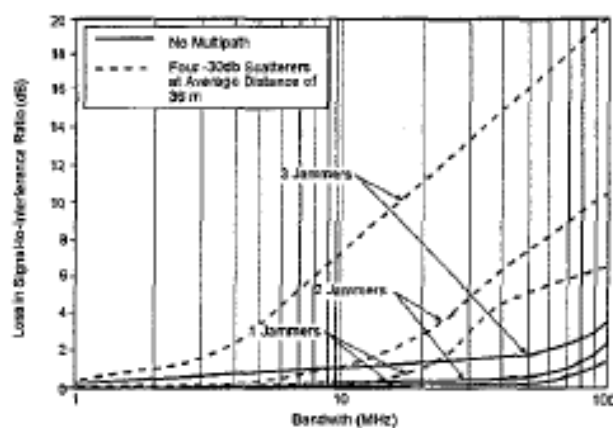


Fig. 2. Effect of multipath on signal-to-interference loss for array that uses spatial degrees of freedom only.

interferers near the horizon the maximum differential delay τ_{\max} between the direct ray and the multipath is $\tau_{\max} = 2\sqrt{2}d/c$, where c is the speed of light. Therefore, in order to compensate for delays of this order we require that the number of time taps P per antenna must satisfy (see Appendix B)

$$(P - 1)T \geq \tau_{\max} \quad (35)$$

For a tap spacing $T = 1/B$ and $d = 30$ m this condition becomes $P > 1 + 0.28B$ (MHz), where B (MHz) is the bandwidth in MHz. Thus, if only one tap is used (i.e., spatial degrees of freedom only) we expect performance to degrade significantly if bandwidth is much larger than a few MHz. In Fig. 2 we show the loss, relative to the interference-free environment, in the adapted signal-to-interference ratio for the cases when the antenna array is illuminated by one, two, and three strong ($J/N = 60$ dB/antenna/interferer) interferer, and multipath is present and absent. Note, that although there is little degradation in system performance in the absence of multipath, as expected, when multipath is present the performance begins to degrade badly for bandwidths exceeding a few MHz. This clearly indicates the need for the adaptive FIR filter behind each antenna, even when the antenna array is perfectly equalized (cancellation ratio = ∞).

We now illustrate for $B = 20$ MHz how adding temporal taps cures the degradation introduced by the multipath. In order to stress the processor we increase the interference-to-noise ratio from 60 dB to 70 dB per element per interferer, but again assume the array is well equalized (cancellation ratio = 120 dB). Also, now the four multipath scatterers are placed randomly⁷ at an average distance of

⁷The scatterers are placed randomly (uniform probability density) within a circular annulus in the same plane as the antenna array. The inner radius of the annulus is $\bar{R} - \Delta R/2$ and its outer radius is $\bar{R} + \Delta R/2$ where $\bar{R} = 12$ meters and $\Delta R = 2$ meters.

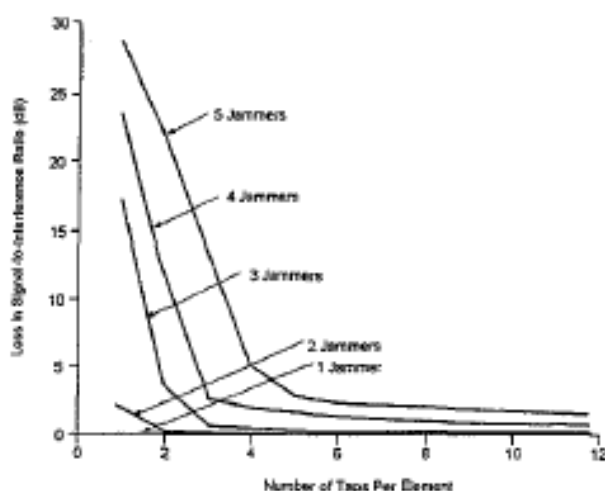


Fig. 3. Illustration that increasing number of time taps decreases loss in signal-to-interference ratio.

12 m from the center of the antenna array, the tap spacing is now $0.84/B$, and the results shown in Fig. 3 are the averages over ten realizations of the multipath scatterer locations. From Fig. 3 we see that, as expected, adding temporal taps does indeed reduce the loss in signal to interference caused by the interference plus multipath. The maximum differential multipath delay is approximately 140 ns so that for $T = 0.84/B$ and $B = 20$ MHz, (35) predicts that $Q \geq 4$ -taps are required. As can be seen from Fig. 3 the signal-to-interference loss is always modest if four or more taps are employed.

B. Effect of Channel Mismatch

Although the results in Fig. 3 are encouraging, we must recognize that they are for a perfectly equalized array. We must now explore how imperfect equalization affects performance. If the antenna pair is illuminated by an interferer that produces an interference-to-noise ratio of 70 dB per element then a cancellation ratio of 20 dB implies that the output interference-to-noise ratio after subtraction is 50 dB. However, an adaptive tapped delay line (i.e., FIR filter) of the type shown in Fig. 1 can dramatically improve the channel equalization. We illustrate this in Fig. 4 where we show the output interference-plus-noise to noise ratio when a pair of antennas operating over a 20 MHz band are illuminated by a broadband interferer that produces an interference-to-noise ratio of 60 dB/element. The results shown are the averages over ten Monte Carlo simulations of the receiver amplitude and phase ripples, for the case when each receiver has three (random) ripples across the 20 MHz passband. Note that, as expected, the adaptive array self-equalizes if sufficient temporal taps (as was the case previously, the tap spacing is $T = 0.84/B$) are employed.

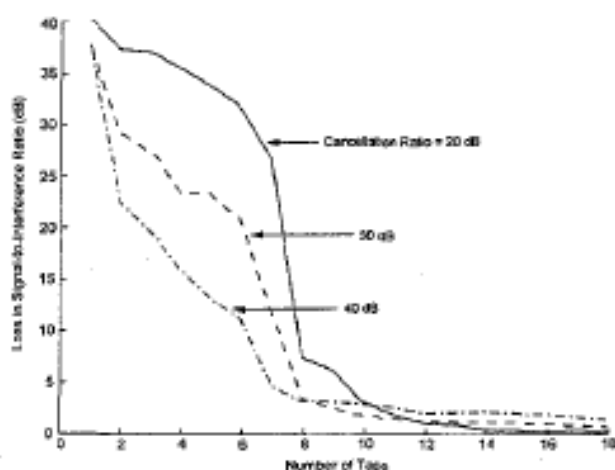


Fig. 4. Illustration of self-equalization by two-element adaptive array.

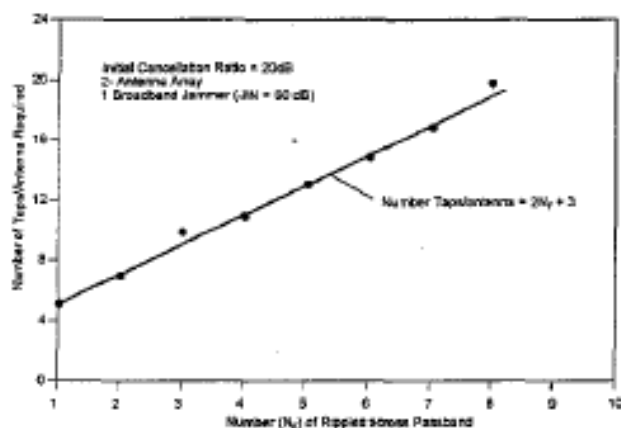


Fig. 5. Self-equalization of two-antenna adaptive array.

We have performed multiple, additional Monte Carlo simulations of the self-equalization⁵ capability of an adaptive array, and some of the results are summarized in Figs. 5 and 6. In Fig. 5 we consider a two-element adaptive array illuminated by a single broadband interferer, and find that the antenna can self-equalize if each antenna contains $2N_r + 3$ taps, where N_r is the number of ripples across the band B in each receiver response function. Note that this is about half the number of taps calculated by Monzingo and Miller [2], because they use an adaptive FIR filter behind only one antenna and we have one behind both antennas.

In Fig. 6 we consider the seven-element circular array illuminated by three broadband interferers located randomly along the horizon ($0 < \text{azimuth} < 2\pi$). For this case only $N_r + 3$ taps per antenna are required. Fewer taps per antenna are required (as compared with the two-element adaptive array) because the seven-element adaptive array has the

⁵We define "self-equalization" as cancellation of the interference to within 3 dB of the receiver noise floor.

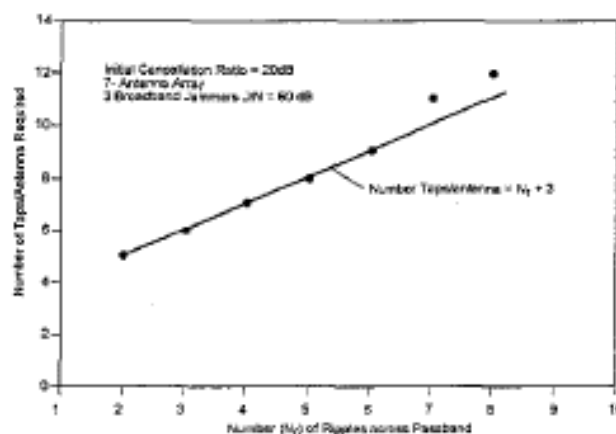


Fig. 6. Self-equalization of seven-antenna adaptive array.

freedom to choose the four or five channels that are best matched to each other, and ignore channels with response functions that are very different from the others (the two-element array doesn't have this luxury).

One should (if possible) choose a receiver technology that has the minimum number of random phase and amplitude ripples across the band B . If the number N_r of ripples is five or fewer it may be feasible to self-equalize. Otherwise a fixed-weight equalization filter is required in each channel.

C. Effect of Steering Vector Mismatch

Because one does not always know the precise angular location of the GPS satellite, it is important to study the sensitivity of the adaptive filter to errors in satellite location. Therefore, we have performed multiple simulations of the loss in output signal-to-interference ratio as a function of the difference between the true satellite location (θ_s, ϕ_s) and our estimate $(\hat{\theta}_s, \hat{\phi}_s)$ of its position, for the case of one to three strong jammers (60 dB/jammer/element) located randomly on the horizon (randomly placed over $0 < \text{azimuth} < 2\pi$) and a GPS satellite located randomly in the upper hemisphere, but not within 15° of the horizon. The mean loss due to steering vector mismatch is summarized in Table I. Observe that as long as the steering-vector mismatch is less than about 15° the loss is tolerable.

D. Distortion Introduced by the Adaptive Filter

In Section IV we discussed the potential effects on the crosscorrelation function introduced by the adaptive FIR filter in Fig. 1. There are a number of issues to be considered. These are: does the adaptive filter produce a bias (time shift) of the cross correlation function peak that is different for different GPS satellite locations (a constant bias

TABLE I
Loss Due to Steering-Vector Mismatch

Angular Error in GPS Direction (degrees)	Loss in S/I (dB)
0	0
5	0.1
10	0.6
15	1.4
20	2.4
25	3.7

that is the same for all satellites does not affect the estimate of position using the GPS system)? Is there significant broadening of the cross correlation, leading to an increase in pseudo-range error? Does the adaptive filter introduce a significant phase error that will affect the estimate of the carrier phase used by high-precision differential GPS systems? We have provided answers to these questions through multiple simulations, using (21) to calculate the cross correlation function for the case when the GPS signal is a PN sequence that has the power spectrum

$$P(f) = \frac{P_0}{B} \text{sinc}^2 \left(\frac{\pi f}{B} \right). \quad (36)$$

If (16) and (36) are substituted into (21), the time origin shifted to the center tap, and the integration performed, we find

$$C(\tau) = P_0 \sum_{k=1}^K \sum_{q=0}^{P-1} \tilde{w}_{kq} \text{tri}(\alpha) \quad (37)$$

where $\text{tri}(x) = 1 - |x|$ for $|x| < 1$, $\text{tri}(x) = 0$ for $|x| > 1$

$$\alpha = B \left[\tau + \frac{\xi_k}{c} + \left[q - \frac{(P-1)}{2} \right] T \right] \quad (38)$$

and $\tau = 0$ corresponds to the delay on the center tap of each delay line.

In Fig. 7 we show a typical result for the normalized cross correlation function $C(\tau)/C(0)$ for the cases when there are one to four, broadband, strong (interference to noise ratio = 60 dB/element/interferer) interferers located randomly in azimuth along the horizon. Also present are four moderate strength (-30 dB) multipath scatterers located randomly near the plane of the antenna at an average range of 14.2 m. From Fig. 7 we note the following points. 1) There is no discernable displacement of the cross correlation peak from its correct location at $\tau = 0$. (In fact, in over 100 different simulations the largest shift we observed was only $0.05/B$.) 2) The cross correlation function has nearly the same shape in the presence of one or two interferers as it does in the interference-free case.⁹

⁹In the absence of interference the normalized crosscorrelation is $1 - B|\tau|$ for $|\tau| < B^{-1}$, and zero for $|\tau| > B^{-1}$.

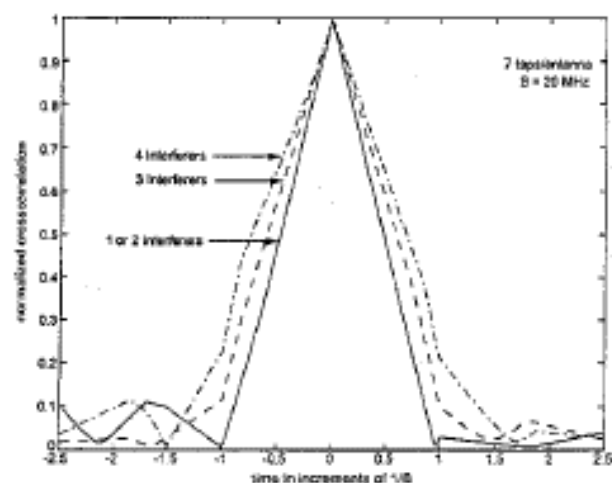


Fig. 7. Uncompensated FIR filter does not significantly affect the cross correlation function.

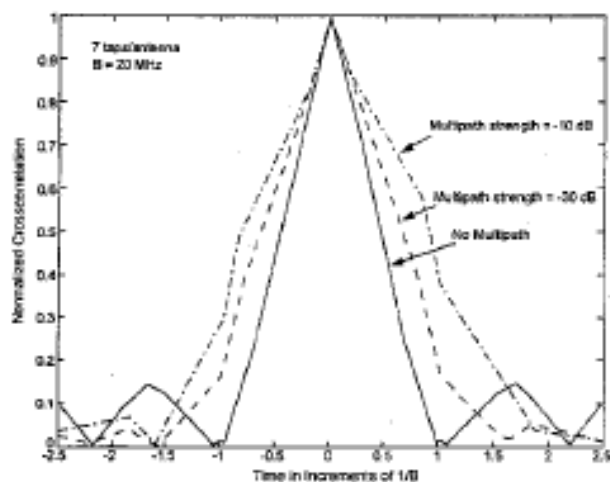


Fig. 8. Cross correlation function is broadened in presence of very strong multipath.

3) Even in the presence of four strong, broadband interferers there is not a drastic broadening of the cross correlation function. Hence, the increase in pseudo-range error is modest.

It is also important to question whether the presence of stronger multipath would modify the above conclusions. Therefore, we varied the strength and location of the multipath scatterers. In Fig. 8 we show results for one of the worst cases encountered. Again the crosscorrelation peak is at the correct location, but for very strong multipath (-10 dB) there is a significant broadening of the cross correlation peak. In general, however, multipath this strong is not usual because -10 dB multipath corresponds to a scatterer with a bistatic radar cross section of 253 m^2 at a range of 14.2 m. Thus, we conclude that the adaptive FIR filter in Fig. 1 does not shift or radically broaden the cross correlation function $C(\tau)$.

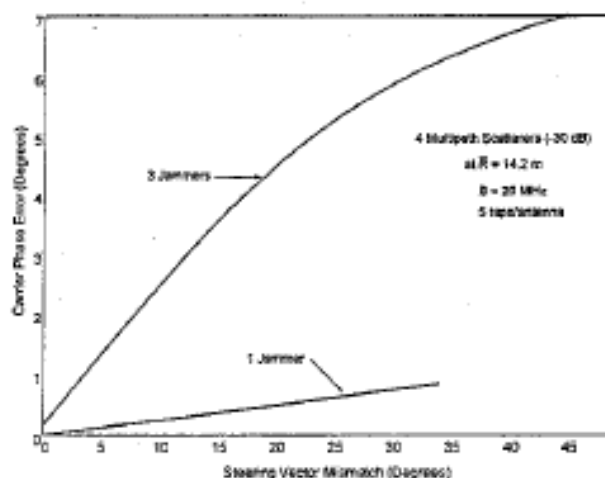


Fig. 9. Steering vector mismatch (degrees).

Consequently there is no range bias error and only a very modest increase in pseudo-range error. The compensation filter $G(f) = H^*(f)$ discussed in (22) is unnecessary.

We also studied the carrier phase error, which is equal to the phase of $C(0)$. Typical values of the carrier phase error are shown in Fig. 9 as a function of steering-vector mismatch, which is the difference between the true GPS satellite location (θ_s, ϕ_s) and its estimated position $(\hat{\theta}_s, \hat{\phi}_s)$. When the steering vector is correctly estimated (mismatch = 0) the carrier phase error is a fraction of a degree. Even for rather crude estimates (errors up to 20°) of the steering vector the carrier phase error is only a few degrees. Thus, it appears that the adaptive FIR filter will not have a deleterious effect on differential GPS systems that employ carrier phase tracking for high-precision position location.

VII. SPACE-TIME VERSUS SUBOPTIMUM SPACE-FREQUENCY PROCESSING

We would now like to compare the performance of the full space-time processor with that of the suboptimum space-frequency processor, using the metric of computational complexity. That is, for equal computational complexity which method produces a lower residual interference after adaptation? The number of real operations per second to form and invert the covariance matrix, using an LU factorization and forward-back substitution, for the full space-time processor is¹⁰ $17.33 (PK)^3 F_u$, where P is the number of time taps and F_u is the weight update rate. The number of operations per second to apply the weights

¹⁰This assumes that $4 PK$ samples are used to estimate the covariance matrix, and that the covariance domain is used. If the QR decomposition is done directly on sampled data then $17.33 (PK)^3 F_u$ is replaced by $32 (PK)^3 F_u$.

in (1) is $(8KP - 2)F_s$, where F_s is the sampling rate, so that the total number of operations per second is the sum of these two quantities.

For suboptimum, space-frequency processing there are $17.33(KQ)^2MF_s$ operations per second to form and invert the covariance matrix, where M is the number of frequency bins and Q is the processing order. For nonoverlapped FFTs we require $(K + 1)(2 + 5\log_2 M)F_s$ operations per second to apply real weights (e.g., Blackman) to the data block (of M samples), do the FFTs for each antenna and then perform an inverse FFT (IFFT). In order to reduce windowing losses, the FFTs are usually overlapped by at least fifty percent. If the FFTs are overlapped by a factor O_v (i.e., $O_v = 1$ means no overlap, $O_v = 2$ means 50% overlap) then there are $O_v(K + 1) \cdot (2 + 5\log_2 M)F_s$ operations per second to do the FFTs and IFFT. Also, there are $(8QK - 2)O_vF_s$ operations per second to apply the weights. Thus, the total number of operations per second is

$$17.33(KQ)^2MF_s + O_vF_s[8KQ - 2 + (K + 1)(2 + 5\log_2 M)].$$

There are now two cases to be considered. In a highly dynamic environment the covariance matrix update rate will dominate the computations count. However, in a less dynamic environment the computation of the FFTs and application of the weights will dominate. Typically, if the weight update rate is less than 1 kHz the weight application will dominate the computations count, so that for space-time processing the number of operations per second is approximately $(8KP - 2)F_s$, and for order Q space-frequency processing the number of operations per second¹¹ is approximately $O_vF_s[8KQ - 2 + (K + 1) \cdot (2 + 5\log_2 M)]$. In the results to follow we assume that the update rate is slower than 1 kHz and that a 50% overlap ($O_v = 2$) is used.

In order to now compare performance versus processing requirements, we consider the scenario where the seven-element circular array is operating over a bandwidth B of 20 MHz and illuminated by zero, one, two and three broadband (bandwidth greater than or equal to 20 MHz) interferers plus multiple narrowband (i.e., bandwidth $\rightarrow 0$) interferers. Each interferer has an interference-to-noise ratio of 70 dB, and there are four multipath scatterers present with

¹¹We can also consider memory requirements. A space-time processor with K antennas and P taps requires each processing chain to collect $4KP$ samples to estimate the covariance matrix, so that the K antenna system has a memory requirement of $4K^2P$ complex. An order 1 space-frequency processor requires each antenna processing chain to collect $4KM$ samples (i.e., $4K$ samples per frequency bin) so that the total memory requirement is $4K^2M$. Thus, the space-frequency processor requires M/P more storage than the space-time processor. Thus, memory requirements favor space-time over space-frequency processing. Ultimately, this data requirement will limit adaptation rates for space-frequency processing by the same M/P ratio relative to space-time processing.

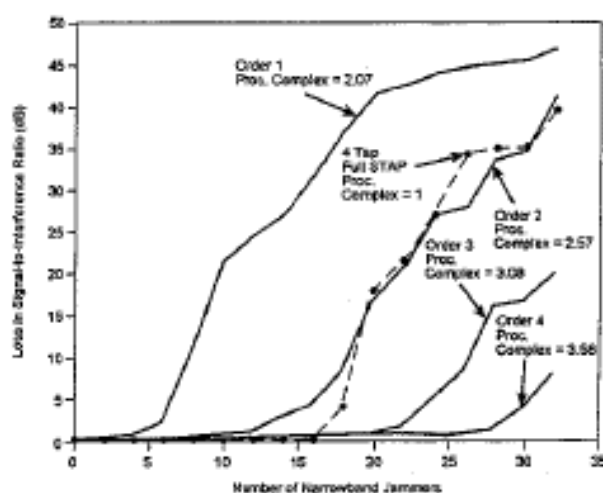


Fig. 10. Comparison of 16 bin space-frequency processing with 4-tap space-frequency processing. One wideband interferer.

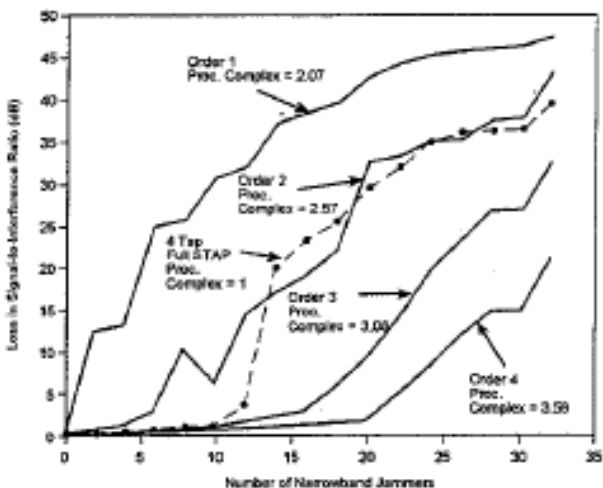


Fig. 11. Comparison of 16 bin space-frequency processing with 4-tap space-time processing. Two wideband interferers.

a strength of -30 dB and an average range of 15 m. The narrowband interferers are randomly located in azimuth at elevations close to the horizon, and are also randomly placed within each frequency bin.

In Figs. 10 and 11 we show the residual interference after adaptation for the case of sixteen bin, suboptimum, space-frequency processing using a Blackman-Harris window. The cancellation ratio for all cases is 120 dB. The results shown are the averages over three realizations of the random placements of the narrowband interferers within the frequency bins. Also shown is space-time processing (STAP) using four time taps. For each curve, we show the relative processing complexity normalized to the processing complexity for 4-tap space-time processing. From Figs. 10 and 11 it is evident that four tap space-time processing outperforms both order 1 and order 2 suboptimum, 16 bin,

TABLE II
Number of Interferers Canceled Without Increasing Noise Floor by More Than 3 dB

Processing Type	Relative Processing Complexity	Number of Interferers Cancelled			
		0 wideband 23 narrowband	1 wideband 14 narrowband	2 wideband 6 narrowband	3 wideband 1 narrowband
Space-Frequency 16 bin, order 2	2.57				
4 Tap Space-Time	1	0 wideband 26 narrowband	1 wideband 17 narrowband	2 wideband 12 narrowband	3 wideband 5 narrowband

space-frequency processing and requires less than one-half the computations. For example, in Table II we compare 4-tap STAP with 16 bin, order 2, space-frequency processing, using the performance measure that there is less than a 3 dB increase in the interference-plus-noise to noise ratio after adaptation. Clearly, space-time is the winner when only sixteen frequency bins are used in the space-frequency processor.

The conclusion does not change if a larger FFT is used. A 64 bin, order 1 space-frequency processor requires 2.79 times the number of computations as a four-tap space-time processor, so let us compare these two approaches. First, consider the scenario where the seven-element array is illuminated by three, randomly located, wideband interferers plus a varying number of narrowband interferers. As before, the cancellation ratio is 120 dB. The interference-plus-noise to noise ratio after adaptation for both processors is shown in Fig. 12, and indicates that the four-tap space-time processor performs as well as the first order 64 bin space-frequency processor with a Blackman-Harris window.

It is important to recognize, however, that the aforementioned conclusions apply to the case when the weight update rate is less than 1 kHz. When the update rate is much faster than 1 kHz the first-order space-frequency processor with 128 or more bins¹² is often superior to the space-time processor (e.g., a 128 point FFT processor gives equal performance using fewer operations per second than the space-time processor when the update rate exceeds 10 kHz).

It is interesting to physically interpret some of the results in Figs. 10–12. Consider the P tap space-time processor. In view of our discussion in Section V that space-time and full-order space-frequency processing

¹²One drawback with large-size FFTs is that the bandwidth of each frequency bin becomes very small (each bin has a bandwidth of B/M where B is the operating bandwidth and m is the FFT size). Thus, in order to estimate the $K \times K$ covariance matrix one requires $4K$ independent samples, which requires a time interval of a $4KM/B$ s. For $K = 7$, $M = 256$, $B = 20$ MHz this requires a time interval of 0.358 ms. Typically, in a dynamic environment the weights will need to be updated once per millisecond, so $M = 256$ is probably an upper limit.

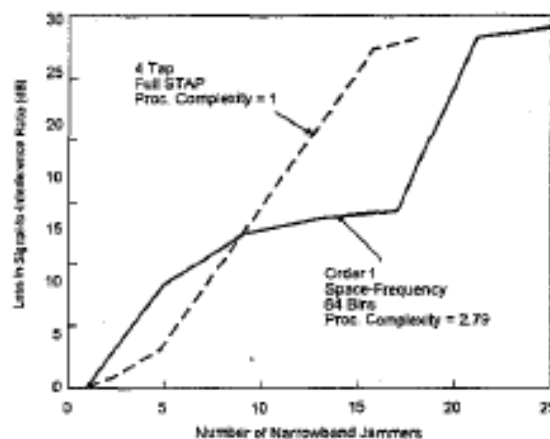


Fig. 12. Comparison of 64 bin space-frequency processing with 4-tap space-time processing. Three wideband interferers.

are equivalent, we can view this space-time processor as a full order, P bin, space-frequency processor. If the processor has K antennas and P bins, there are $KP - 1$ degrees of freedom available. The desired GPS signal is broadband, spreading across all P frequency bins. Thus, in each bin one spatial degree of freedom is required to protect the signal. Each broadband interferer also requires one spatial degree of freedom in each bin in order to place a null on that interferer. This leaves a total of

$$\begin{aligned}
 N_0 &= KP - 1 - P - NP \\
 &= (K - N - 1)P - 1
 \end{aligned} \tag{39}$$

degrees of freedom to cancel narrowband interferers, where N is the number of broadband interferers. For $K = 7$ antennas, $P = 4$ bins, and $N = 1$ broadband interferer we see from (39) that, in theory, the processor can cancel up to $N_0 = (7 - 2)4 - 1 = 19$ narrowband interferers. From Fig. 10 we see that because of frequency overlap and because multipath is also present, one can't quite cancel nineteen narrowband interferers down to the noise floor, but it is possible to cancel sixteen or seventeen narrowband interferers down to near the noise floor. Likewise, for $N = 2$ broadband interferers, (39) predicts that 15 narrowband interferers can also be canceled, whereas the simulation in Fig. 11 indicates that eleven or

twelve are actually canceled down to near the noise floor.

The low-order ($Q = 1, 2$) suboptimum space-frequency processor doesn't perform as well as hoped because of leakage from bin to bin, even when a Blackman-Harris window (which has extremely low sidelobes) is used. The problem is that, although the window reduces the sidelobes, it spreads the mainlobe frequency response over multiple bins. Consequently, a narrowband interferer in frequency bin m has strong leakage into bins $m \pm 1$, $m \pm 2$ so that spatial nulls are required in all five bins to null the single narrowband interferer. Thus, the available degrees of freedom are rapidly consumed. Other windows, such as the Hamming window, fare no better. Although, not presented here, we also studied the use of polyphase filters to alleviate this leakage problem, but had limited success.

VIII. SUMMARY

We have demonstrated that by using a space-time processor the interference from multiple, strong interferers plus their multipath can be canceled down close to the noise floor without producing serious loss or distortion of a GPS signal. We also found that the processor demonstrates a remarkable capability for self-equalization. An approximate relationship for the number of broadband (N) and narrowband (N_0) interferers that can be canceled is

$$N_0 + NP \simeq (K - 1)P - 1 \quad (40)$$

where P is the number of time taps used behind each antenna in Fig. 1 and K is the number of antennas. The result above assumes that the wideband interferers occupy the entire operating band B and that the narrowband interferers are randomly located across B . The number of time taps must satisfy

$$(P - 1)T > \tau_{\max} \quad (41)$$

where T is the time-tap spacing, which must be less than $1/B$ and τ_{\max} is the maximum differential time delay between the direct interferer ray and the multipath.

Previously, we speculated that suboptimum space-frequency adaptive processing would work nearly as well as space-time processing, but would require fewer computations. We have found that this speculation is untrue unless the weights need to be updated very rapidly. For moderate update rates the space-time processor outperformed the suboptimum space-frequency processor of equal computational complexity. However, we also studied the case when the weights needed to be updated very rapidly (e.g., once per 100 μ s) so that the weight update begins to dominate the computations count. In this case the space-time and space-frequency (with FFT size > 64) processors both gave roughly equal performance

for equal computations count. Thus, space-time is not always a clear winner, and if the update rate is sufficiently rapid (e.g., roughly 10 kHz or faster) the first-order space-frequency processor with 128 or 256 bins outperforms the space-time processor.

Although all results presented here employed ideal covariance matrices, we also performed some simulations using estimated covariance matrices (using four times the number of degrees of freedom samples of the voltages for the estimate) and obtained essentially the same results.

APPENDIX A. INTERFERENCE COVARIANCE MATRIX

In this Appendix we calculate the interference covariance matrix. Consider an array of K antennas mounted on an arbitrary platform and suppose the position of antenna k is (x_k, y_k, z_k) , and that multipath is represented by L point scatterers with scatterer p having a bistatic scattering function¹³ given by $S_p(\theta_s, \phi_s; \theta_i, \phi_i)$, where (θ_i, ϕ_i) is the angular direction of the incident radiation and (θ_s, ϕ_s) is the angular direction of the scattered radiation. This array is illuminated by N far-field interferers such that interferer n produces a voltage $j_n(t) \exp(i2\pi f_0 t)$ on the reference element of the antenna array in the absence of multipath, where f_0 is the carrier frequency. Then, if both the direct and multipath voltages are included (and polarization effects are temporarily ignored) the voltage produced by the N interferers on antenna element k , after downconversion (by multiplying by $\exp(-i2\pi f_0 t)$) is¹⁴

$$y_k(t) = \sum_{n=1}^N j_n(t - \tau_{nk}) \exp(-i2\pi f_0 \tau_{nk}) + \sum_{n=1}^N \sum_{p=1}^L b_{kp} S_p(\theta_k, \phi_k; \theta_n, \phi_n) j_n(t - \tilde{\tau}_{np} - T_{pk}) \times \exp[-i2\pi f_0 (\tilde{\tau}_{np} + T_{pk})] + u_k(t) \quad (42)$$

where τ_{nk} is the direct-path delay at antenna k from interferer n , $\tilde{\tau}_{np}$ is the delay from interferer n to scatterer p , T_{pk} is the delay from scatterer p to antenna k , b_{kp} is a term that contains the range from scatterer p to antenna k and $u_k(t)$ is the receiver noise on

¹³The bistatic radar cross section is $|S_p|^2$.

¹⁴The result in (42) ignores mutual coupling between antennas. This can be approximately included by writing

$$y'_k(t) = y_k(t) + \sum_{l \neq k} \rho_{kl} j_l(t - \xi_{kl})$$

where ρ_{kl} is a complex coupling coefficient and ξ_{kl} is the propagation delay from antenna k to antenna l . We have included mutual coupling in our covariance matrix, but our calculations indicate that it has a negligible effect on the results unless $|\rho| > -15$ dB, which represents a highly coupled antenna array. For a detailed treatment of the effect of mutual coupling on adaptive arrays the reader can consult [21].

antenna k . In the frequency domain we can write (42) as

$$Y_k(f) = \sum_{n=1}^N J_n(f) G_{nk}(f) + U_k(f) \quad (43)$$

where Y_k , J_n , and U_k , are the Fourier transforms of y_k , j_n , and u_k , respectively, and

$$G_{nk}(f) = \exp[i2\pi(f - f_0)\tau_{nk}] + \sum_{p=1}^L b_{kp} S_p \exp[i2\pi(f - f_0)(\tau_{np} + T_{pk})]. \quad (44)$$

Because the channels in the antenna array are not perfectly equalized, we must account for the different frequency response of each channel across the band of operation. We include this effect by defining $H_k(f)$ as the frequency response of receiver k , so that the interference voltage at the output of receiver k is

$$V_k(f) = H_k(f) Y_k(f). \quad (45)$$

Then, the time domain interference on time tap q of antenna k (see Fig. 1) is

$$v_k(t - qT) = \sum_{n=1}^N \int_{-\infty}^{\infty} df H_k(f) J_n(f) G_{nk}(f) \times \exp[i2\pi f(t - qT)] + \tilde{u}_k(t - qT) \quad (46)$$

where $\tilde{u}_k(t - qT)$ is the noise on time tap q of antenna k .

Let us now derive the interference covariance matrix for the case when the interference consists of N_1 monochromatic (i.e., very narrowband) interferers and N_2 statistically independent, stationary, broadband noise interferers. For a monochromatic noise interferer radiating a frequency f_n we have

$$J_n(f) = J_n \delta(f - f_n) \quad (47)$$

and for the independent, wideband noise interferers we have

$$\langle J_n(f) J_m^*(f') \rangle = P_n(f) \delta_{nm} \delta(f - f') \quad (48)$$

where $P_n(f)$ is the power spectrum for interferer n , and δ_{nm} is the Kronecker delta. Thus, by using (47) and (48) we can show that the general term in the covariance matrix is

$$\begin{aligned} R_{kl}(p - q) &= \langle v_k(t - pT) v_l^*(t - qT) \rangle \\ &= \sum_{n=1}^{N_1} \bar{P}_n H_k(f_n) H_l^*(f_n) G_{nk}(f_n) G_{nl}^*(f_n) \\ &\quad \times \exp[i2\pi f_n(q - p)T] \\ &\quad + \sum_{n=1}^{N_2} \int_{-\infty}^{\infty} df P_n(f) H_k(f) H_l^*(f) G_{nk}(f) G_{nl}^*(f) \\ &\quad \times \exp[i2\pi f(q - p)T] + \delta_{kl} R_N[(p - q)T] \quad (49) \end{aligned}$$

where $\bar{P}_n = |J_n|^2$ and

$$R_N[(p - q)T] = \langle \tilde{u}_k(t - pT) \tilde{u}_k^*(t - qT) \rangle \quad (50)$$

is the noise covariance.

The response $H_k(f)$ of channel k can be written as

$$H_k(f) = [1 + \alpha_k(f)] \exp[i\beta_k(f)]. \quad (51)$$

The phase fluctuation β_k from channel-to-channel (the mean group delay has been removed from (51)) is usually small in comparison with unity, so that the exponential can be expanded in a Taylor series giving

$$H_k(f) = 1 + a_k(f) + \dots \quad (52)$$

where $a_k = \alpha_k + i\beta_k$. Typically, $a_k(f)$ can be represented as

$$a_k(f) = b_k f + c_k \sin(2\pi\gamma_k f + \phi_k) \quad (53)$$

where the first term on the right-hand side of (53) is the differential variation that is linear in frequency and the second term represents a ripple across the passband that also varies from channel-to-channel. In general, the coefficients b_k and c_k may be complex, but γ_k and ϕ_k are real. If (53) is used in (49) the integration over frequency is readily performed, but the results are omitted here.

The cancellation ratio is a measure of the mismatch from antenna to antenna. For a white-noise jammer illuminating antennas k and ℓ the cancellation ratio in decibels is defined as $-10 \log_{10}(CR)$ where

$$CR = \frac{(|v_k(t) - v_\ell(t)|^2)}{P_j B} \quad (54)$$

If (53) is used in (46) and the resulting expression substituted into (54) we find

$$CR = CR' + CR'' \quad (55)$$

where CR' is the contribution to the cancellation ratio by the linear fluctuations from channel to channel, and CR'' is the contribution due to the differential ripples across the passband. If the real and imaginary parts of the coefficient b_k are random and uniformly distributed between $\pm b_{\max}$ we find that

$$CR' = \frac{B^2}{9} b_{\max}^2. \quad (56)$$

Also, if ϕ_k is random and uniformly distributed between 0 and 2π and the real and imaginary parts of the coefficient c_k and each random and uniformly distributed between $\pm c_{\max}$ we find

$$CR'' = \frac{2}{3} c_{\max}^2. \quad (57)$$

Typically, it is very easy to equalize the variations that are linear in frequency, but it is much more difficult to equalize multiple ripples across the passband. Thus, the value of CR'' is much more important than the value of CR' .

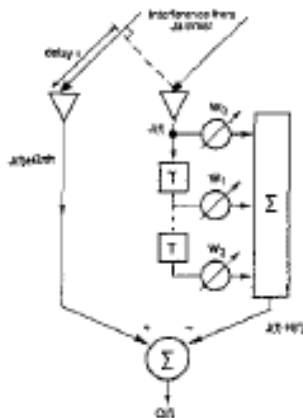


Fig. 13. Two-element processor.

It should be noted that the Doppler effects due to either moving interferers or a moving platform are not included in this analysis. We have shown that Doppler effects can be ignored if

$$2\pi f_d(P-1)T \ll 1 \quad (58)$$

where f_d is the Doppler shift (differential speed divided by wavelength) and P is the total number of taps in each delay line. For all of the cases considered in this analysis the condition in (58) is easily satisfied.

APPENDIX B. NUMBER OF TIME TAPS REQUIRED

In order to better understand the condition expressed by (35) suppose we have the two antenna configuration shown in Fig. 13, and this configuration is illuminated by an interferer at an angle θ , so that the delay between the two antennas is $\tau = d \sin \theta / c$. We now desire to examine how well the tapped delay line can track the delay across the frequency band. If the interferer voltage has a Fourier transform $J(f)$ then the output $O(f)$ in Fig. 13 is

$$O(f) = J(f)[\exp(i2\pi f\tau) - H(f)] \quad (59)$$

where

$$H(f) = \sum_{q=0}^{P-1} w_q \exp(i2\pi qfT). \quad (60)$$

If we use Parseval's Theorem, we can express the mean output power as

$$\epsilon^2 = \int_{-\infty}^{\infty} df P_f(f) |\exp(i2\pi f\tau) - H(f)|^2 \quad (61)$$

where $P_f(f)$ is the interferer power-spectral-density. If we assume the interferer radiates white noise, so that $P_f(f) = P_f$ for $|f| < B/2$ and $P_f = 0$, otherwise, we can

write (61) as

$$\begin{aligned} \frac{\epsilon^2}{P_f B} &= 1 - \sum_{q=0}^{P-1} (w_q + w_q^*) \text{sinc } \pi B(\tau - qT) \\ &+ \sum_{q=0}^{P-1} \sum_{r=0}^{P-1} w_q w_r^* \text{sinc } \pi B(q-r)T. \end{aligned} \quad (62)$$

If we minimize ϵ^2 with respect to w_q we find that the normalized residual power after adaptation is

$$\text{residue} = 1 - h^T \Gamma^{-1} h \quad (63)$$

where h is $P \times 1$ vector with components

$$h_q = \text{sinc } \pi B(\tau - (q-1)T) \quad (64)$$

and Γ is a $P \times P$ matrix with components

$$\Gamma_{qr} = \text{sinc } \pi B T(q-r). \quad (65)$$

A plot of the residue power versus the normalized delay $B\tau$ that must be matched is shown in Fig. 14, for the case when the normalized tap spacing $BT = 0.8$. For the tapped delay line with five taps, the total normalized delay encompassed is $(P-1)BT = 3.2$. Note that as long as $B\tau \leq 3.2$ the normalized interferer residue is small, but for $B\tau > 3.2$ it rises rapidly. When nine taps are used the total delay encompassed is $(P-1)BT = 6.4$, and as long as $B\tau \leq 6.4$ the interferer residue is small, but for $B\tau > 6.4$ the residue rises rapidly, because the delay line is not long enough to match the delay.

APPENDIX C. INCLUSION OF POLARIZATION

The effects of polarization are readily included in our analysis. In order to do so, let us define a 2×1 vector J_n as

$$J_n^T = [J_{nH}(t) \quad J_{nV}(t)] \quad (66)$$

where J_{nH} and J_{nV} are, respectively, the voltages emitted by interferer n on horizontal and vertical polarization. Also define the 2×1 -vector α_k as

$$\alpha_k^T = [\alpha_H(k) \quad \alpha_V(k)] \quad (67)$$

where $\alpha_H(k)$, $\alpha_V(k)$ are the voltage gains of antenna k on horizontal and vertical polarization, respectively. Finally, define the 2×2 scattering matrix

$$S_p = \begin{bmatrix} S_{HH}(p) & S_{HV}(p) \\ S_{VH}(p) & S_{VV}(p) \end{bmatrix} \quad (68)$$

where s_{HH} , s_{HV} , s_{VH} , s_{VV} are the scattering amplitudes of multipath scatterer p . Then, in place of (42) we can write the general expression for the interference

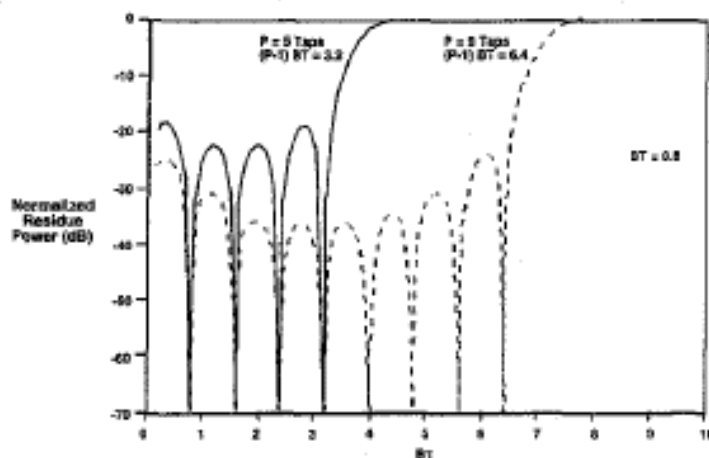


Fig. 14. Normalized residue power for $BT = 0.8$.

voltage received on antenna k as

$$\begin{aligned}
 y_k(t) = & \sum_{n=1}^N \alpha_k^n J_n(t - \tau_{nk}) \exp(-i2\pi f_0 \tau_{nk}) \\
 & + \sum_{n=1}^N \sum_{p=1}^L b_{kp} \alpha_k^n S_p J_n(t - \tilde{\tau}_{np} - T_{pk}) \\
 & \times \exp[-i2\pi f_0(\tilde{\tau}_{np} + T_{pk})] + u_k(t). \quad (69)
 \end{aligned}$$

All of the remainder of the analysis then proceeds exactly as in Appendix A.

It is important that polarization be included in the analysis, because interferers may radiate independent voltages on each of two orthogonal polarizations. In this case, depending on the differences in the crosspolarization response from antenna to antenna, it may take up to twice the number of degrees of freedom to cancel the interferers than it does for interferers that do not use independent signals.

ACKNOWLEDGMENTS

We are grateful to Tom Hopkinson for his leadership on this project and for many useful suggestions. Thanks are also due to Jose Torres, Dan Moulin, Bob DiPietro, Jonathan Williams, B. Rama Rao, and Dan Boschen for valuable discussions.

REFERENCES

- [1] Paulraj, A. J., and Pappas, C. B. (1997) Space-time processing for wireless communications. *IEEE Signal Processing Magazine* (Nov. 1997), 49–83.
- [2] Monzingo, R., and Miller, T. (1980) *Introduction to Adaptive Arrays*. New York: Wiley, 1980.
- [3] Fante, R., and Torres, J. (1995) Cancellation of diffuse jammer multipath by an airborne adaptive radar. *IEEE Transactions on Aerospace and Electronic Systems*, 31 (1995), 805–820.
- [4] Techau, P., Guerci, J., Slowcomb, T., and Griffiths, L. (1999) Performance bounds for interference mitigation in radar systems. In *Proceedings of the 1999 IEEE Radar Conference* (1999), 12–17; ISBN: 0-7803-4977-6.
- [5] Techau, P. (1999) Effects of receiver filtering on hot clutter mitigation. In *Proceedings of the 1999 IEEE Radar Conference* (1999), 84–89; ISBN: 0-7803-4977-6.
- [6] Marshall, D., and Gabel, R. (1996) Simultaneous mitigation of multipath jamming and ground clutter. In *Proceedings of the Adaptive Sensor Array Processing (ASAP) Workshop*, Mar. 1996, report ASAP-4, MIT Lincoln Laboratory.
- [7] Ward, J. (1994) Space-time adaptive processing for airborne radar. Technical report 1015, MIT Lincoln Laboratory, Dec. 1994.
- [8] Brennan, L., Mallett, J., and Reed, I. (1976) Adaptive arrays in airborne MTI radar. *IEEE Transactions on Antennas and Propagation*, AP-24 (1976), 607–615.
- [9] Compton, R. (1988) *Adaptive Antennas*. Englewood Cliffs, NJ: Prentice Hall, 1988.
- [10] Hudson, J. (1989) *Adaptive Array Principles*. London: Peter Peregrinus, 1989.
- [11] VanVeen, B. (1992) Minimum variance beamforming. In S. Haykin and A. Steinhardt (Eds.), *Adaptive Radar Detection and Estimation*. New York: Wiley, 1992.
- [12] Brennan, L., and Reed, I. (1973) Theory of adaptive radar. *IEEE Transactions on Aerospace and Electronic Systems*, AES-9 (1973), 237–252.
- [13] Farina, A. (1992) *Antenna-Based Signal Processing Techniques for Radar Systems*. Boston: Artech House, 1992.
- [14] Hildebrand, F. (1965) *Methods of Applied Mathematics*, 2nd ed. Englewood Cliffs, NJ: Prentice-Hall, 1965.

- [15] Kaplan, E. (Ed.)
Understanding GPS: Principles and Applications.
Boston: Artech House, 1996.
- [16] Parkinson, B., and Spilker, J. (Eds.) (1996)
Global Positioning System: Theory and Applications.
Washington, DC: American Institute of Aeronautics and
Astronautics, 1996.
- [17] Weill, L. B. (1997)
Conquering multipath: The GPS accuracy battle.
GPS World (Apr. 1997), 59–66.
- [18] DiPietro, R. (1992)
Extended factored space-time processing for airborne
radar systems.
In *Proceedings of the 26th Asilomar Conference on Signals,
Systems and Computing* (1992), 425–430.
- [19] Compton, R. (1988)
The relationship between tapped delay line and FFT
processing in adaptive arrays.
IEEE Transactions on Antennas and Propagation, 36
(1988), 15–26.
- [20] Fante, R., and Vaccaro, J. (1998)
Cancellation of jammers and jammer multipath in a GPS
receive array.
Technical report MTR98B0000084, The MITRE Corp.,
Nov. 1998.
- [21] Gupta, I., and Ksienski, A. (1983)
Effect of mutual coupling on the performance of adaptive
arrays.
IEEE Transactions on Antennas and Propagation, 31
(1983), 785–791.